Proc. Estonian Acad. Sci. Eng., 2000, **6**, 3, 186–197
https://doi.org/10.3176/eng.2000.3.02

A MODEL FOR CYCLIC SHEAR IN PLASTICITY

Kalju KENK

Department of Machine Science, Tallinn Technical University, Ehitajate tee 5, 19086 Tallinn, Estonia; kenk@meo.ttu.ee

Received 13 February 1998, in revised form 7 March 2000

Abstract. A model for describing the plastic behaviour of a material in cyclic shear is proposed. It comprises a set of elements connected in parallel, each of which is built up of a linear spring and viscosity and slip subelements, all connected in series. Appropriate choice of subelement properties enables us to describe cyclic hardening and ratchetting processes of the material without the use of the hypothesis of kinematic hardening. The capabilities of the model are illustrated with numerical simulation results.

Key words: plasticity, structural model, cyclic shear.

1. INTRODUCTION

The complexity of material behaviour in cyclic plasticity induces the use of structural models with a finite or infinite number of elements [1,2].

It might seem that an infinite number of elements enables one to describe the deformation process more adequately. However, in practice the calculations are carried out with the use of a finite number of model elements [2]. To determine the necessary parameters of a model, an approximation of the strain–stress diagram obtained with one-dimensional active loading is usually employed.

It is important to choose and determine element characteristics of the model to provide:

1) an adequate strain–stress diagram of the one-dimensional active loading,

2) a sufficiently exact strain–stress diagram of the one-dimensional loading-unloading-reloading process (including ratchetting [3]),

3) a description of the actual response of the material in the one-dimensional reversed cyclic loading.

Such loadings make up part of the model proof tests. In fact, only after proving the validity of the description in these simple cases, it is reasonable to study the complicated multi-axial loading–deformation behaviour. To describe cyclic hardening and ratchetting processes, commonly, the aim is to compose a

model in which each element exhibits both isotropic and kinematic hardening. To consider the isotropic hardening of an element, a scalar parameter is needed; but for kinematic hardening, a tensor (back-stress tensor) has to be determined. Naturally, the determination of the tensor for each element, using only an approximation of the stress–strain curve in one-dimensional active loading, seems very dubious. Therefore at least some supplementary tests are needed.

In [2], Chiang and Beck proposed a model (the C–B model), where the yield surface of an element is totally invariant in the stress space of this element. Thus, neither kinematic hardening rule nor the back-stress tensor are needed in the C–B model. The main advantages of this model are structural simplicity and a small number of element characteristics. However, in spite of rejecting the kinematic hardening rules, the authors show that this model is usually applicable for describing the behaviour of a material even in the case of multiaxial loading. Because the C–B model for the one-dimensional case is based on Masing's hypothesis, it cannot describe cyclic hardening and ratchetting processes. Thus, another model is required.

To describe these processes in cyclic shear, a modified C–B model is proposed in this paper.

2. SOME PROPERTIES OF THE C–B MODEL

According to the C–B model, the deformation process is controlled by the total strain. As the deformation process in tests is usually governed by stress, it is essential to find out whether the C–B model is equivalent to any kinematic hardening model. The most appropriate mode for experimenting is to load a thin-walled tube with tension and torsion. In this case only stresses $\sigma_{11}, \sigma_{12}, \sigma_{21}$ and strains $e_{11}, e_{22}, e_{33}, e_{12}, e_{21}$ are to be considered and for the ith element of the C–B model we obtain the following relations:

1) in the elastic range

$$\mathrm{d}\sigma_{11}(i) = E\mathrm{d}e_{11}, \tag{1}$$

$$\mathrm{d}\sigma_{12}(i) = \frac{E}{1+\nu}\mathrm{d}e_{12}, \tag{2}$$

2) in the plastic range

$$\mathrm{d}\sigma_{11}(i) = E\left[\mathrm{d}e_{11} - 2\sigma_{11}(i)\mathrm{d}\lambda(i)\right], \tag{3}$$

$$\mathrm{d}\sigma_{12}(i) = \frac{E}{1+\nu}\left[\mathrm{d}e_{12} - 3\sigma_{12}(i)\mathrm{d}\lambda(i)\right], \tag{4}$$

$$\mathrm{d}\lambda(i) = \frac{(1+\nu)\sigma_{11}(i)\mathrm{d}e_{11} + 3\sigma_{12}(i)\mathrm{d}e_{12}}{2\sigma_{11}^2(i)(1+\nu) + 9\sigma_{12}^2(i)}, \tag{5}$$

where Young's modulus E, Poisson's ratio ν and Mises yield condition

$$\sigma_{11}^2(i) + 3\sigma_{12}^2(i) - k_i^2 = 0 \tag{6}$$

are used and k_i denotes the tension yield stress of the ith element. To derive Eqs. (3) to (5), the relations

$$\begin{aligned} \mathrm{d}e_{22}^e(i) &= \mathrm{d}e_{33}^e(i) = -\nu \mathrm{d}e_{11}^e(i), \\ \mathrm{d}e_{22}^p(i) &= \mathrm{d}e_{33}^p(i) = -\frac{1}{2}\mathrm{d}e_{11}^p(i), \end{aligned} \tag{7}$$

were taken into account. Here, the superscripts e and p denote elastic and plastic strains, respectively.

As shown in [2], in all the cases of loading considered by the authors, the assumed model, comprising only ten elements, proved to be sufficiently correct to describe material behaviour.

In the following numerical calculations, the dimensionless initial yield stresses $\bar{k}_i(0)$ of the elements and other parameters are taken equal to the ones used in [2]:

$$\bar{k}_1(0) = 0.2638,\ \bar{k}_2(0) = 0.4601,\ \bar{k}_3(0) = 0.6097,\ \bar{k}_4(0) = 0.7448,\ \bar{k}_5(0) = 0.8767,$$

$$\bar{k}_6(0) = 1.0128,\ \bar{k}_7(0) = 1.1612,\ \bar{k}_8(0) = 1.3347,\ \bar{k}_9(0) = 1.5630,\ \bar{k}_{10}(0) = 1.9732,$$

$$\bar{k}_i(0) \equiv k_i(0)/\sigma_{\mathrm{u}}, \qquad \sigma_{\mathrm{u}} = 207 \text{ MPa},\ \ E = 115 \text{ GPa},\ \ \nu = 0.33.$$

The total stresses can be expressed as

$$\sigma_{11} = \frac{1}{10}\sum_{i=1}^{10}\sigma_{11}(i), \quad \sigma_{12} = \frac{1}{10}\sum_{i=1}^{10}\sigma_{12}(i). \tag{8}$$

Using the flow diagram presented in [2] for obtaining the stress response of the model, we have calculated the subsequent yield surfaces of the elements. Each prestrain was followed by partial unloading and then by reloadings along many different straight lines in the strain space. In each reloading, the yield stresses of elements were registered and the subsequent yield surfaces in the total stress space were plotted, using the computed results.

The following three prestraining trajectories in the total strain plane $e_{11}e_{12}$ were considered:

1) the straight line trajectory

$e_{11} = 0$, e_{12} increases from 0 to 0.005 and then decreases to 0.00125,

2) the stepwise trajectory

at the first step $e_{12} = 0$, e_{11} increases from 0 to 0.00035,

at the second step $e_{11} = 0.00035$, e_{12} increases from 0 to 0.005,

3) the stepwise trajectory

at the first step $e_{11} = 0$, e_{12} increases from 0 to 0.002,

at the second step $e_{12} = 0.002$, e_{11} increases from 0 to 0.005.

For a series of different prestrains along the above-mentioned trajectories, Figs. 1a, 2a, and 3a show the corresponding subsequent yield surfaces in the total stress space for an element featured by the smallest initial yield stress. As these surfaces represent the motion of the yield surface of the material in the classical theory of plasticity, we can see that according to the C–B model, in general, the yield surface is subject to pure translation, i.e.,

$$(\sigma_{11} - \alpha)^2 + 3(\sigma_{12} - \beta)^2 = k_1^2(0). \tag{9}$$

Using an approximation of the computed surfaces by Eq. (9), the values of the centre coordinates α and β were determined. The diagrams in Figs. 1b, 2b, and 3b show that the movement of the yield surface centre depends on material deformation prehistory in a very complex way. Thus, as a substantial advantage, the C–B model does not require any kinematic hardening rules. Therefore, to describe the cyclic hardening and ratchetting behaviour of a material, a modification of the C–B model seems to be necessary. In Fig. 4, the dashdot line represents the C–B model strain–stress diagram for copper in active loading by torsion. It appears that the hardening of the material takes place until all the elements are switched on into plastic deformation and starting from strain value ~0.005, the ideal flow follows.

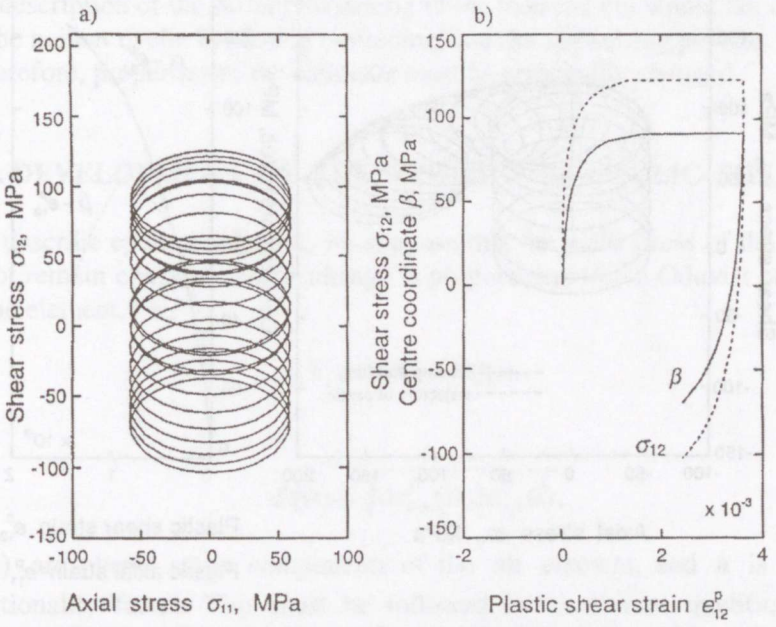

Fig. 1. Yield surface motion for the prestrains along the straight line trajectory: $e_{11} = 0$, e_{12} increases from 0 to 0.005 with prestrain step 0.00025, after that e_{12} decreases with the step 0.00025 until $e_{12} = 0.00125$; a) subsequent yield surfaces, b) dependence of σ_{12} and β on e_{12}^p.

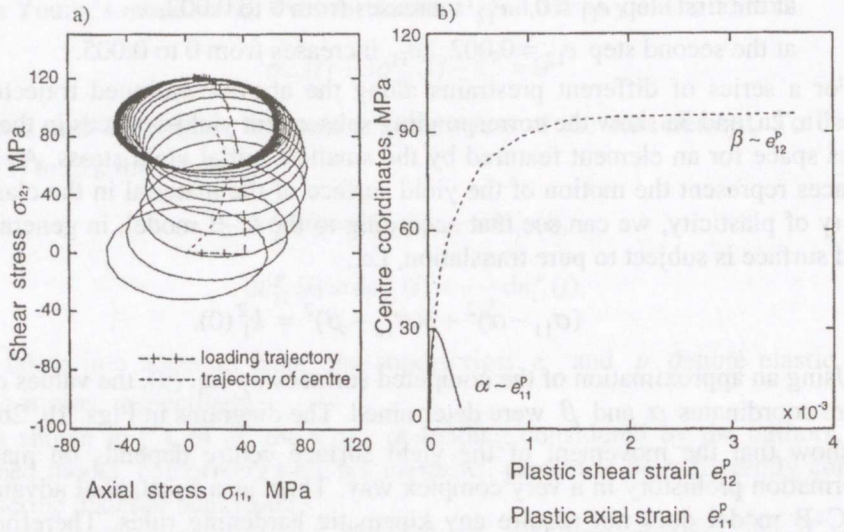

Fig. 2. Yield surface motion for the prestrains along the stepwise trajectory: at first e_{11} increases from 0 to 0.00035, after that e_{12} increases from 0 to 0.005 with step 0.00025; a) subsequent yield surfaces, b) dependence of α and β on e^p_{11} and e^p_{12}, respectively.

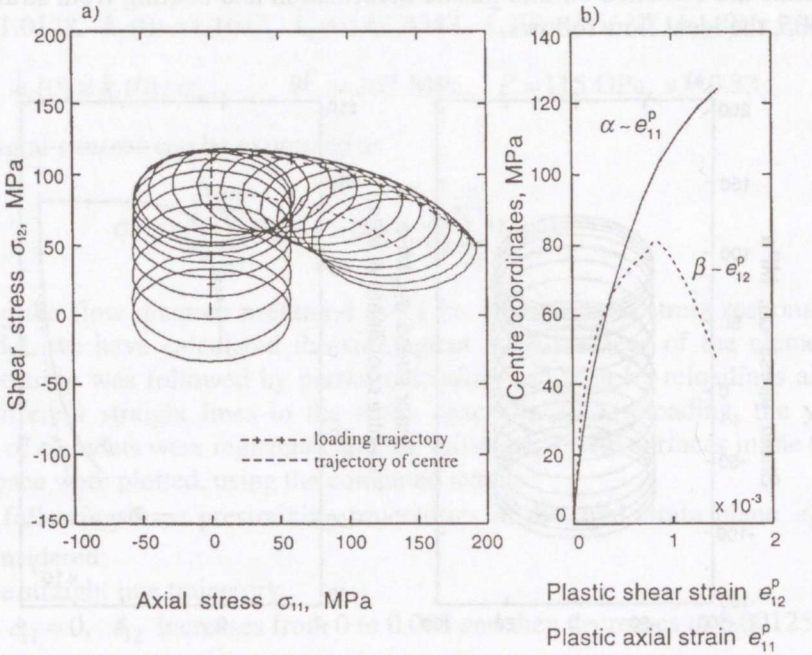

Fig. 3. Yield surface motion for the prestrains along the stepwise trajectory: at first e_{12} increases from 0 to 0.002 with step 0.00025, after that e_{11} increases from 0 to 0.005 with step 0.00025; a) subsequent yield surfaces, b) dependence of α and β on e^p_{11} and e^p_{12}, respectively.

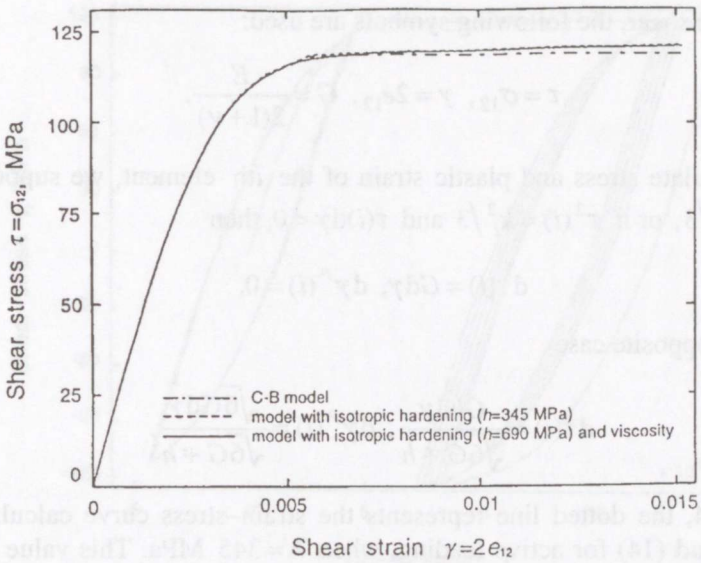

Fig. 4. Strain–stress diagrams for active loading.

From the test diagram (Fig. 8c in [2]), it may be concluded that minor linear hardening will continue even when the strains exceed 0.005. Addition of supplementary elements with higher yield stresses into the C–B model can lead to the description of the further hardening of the material but would not enable to describe neither cyclic hardening (softening) nor the ratchetting process.

Therefore, properties of the elements must be principally changed.

3. DEVELOPMENT OF THE MODEL FOR CYCLIC SHEAR

To describe cyclic hardening, we suppose that the yield stress of the element will not remain constant and its change is proportional to the Odqvist parameter η of the element, i.e.,

$$k_i = k_i(0) + h\eta(i), \tag{10}$$

where

$$\mathrm{d}\eta(i) = \sqrt{\mathrm{d}e^P_{mn}(i)\,\mathrm{d}e^P_{mn}(i)}, \tag{11}$$

$\mathrm{d}e^P_{mn}(i)$ are plastic strain components of the ith element, and h is a scalar proportionality factor. This must be followed by a relevant modification of Eqs. (3) to (5). First, the model has to be modified for the one-dimensional case. Therefore in this paper only cyclic shear will be considered. Modification applicable to the multidimensional case is not covered in this paper.

For pure shear, the following symbols are used:

$$\tau = \sigma_{12},\ \gamma = 2e_{12},\ G = \frac{E}{2(1+\nu)}. \tag{12}$$

To calculate stress and plastic strain of the ith element, we suppose that if $\tau^2(i) < k_i^2/3$, or if $\tau^2(i) = k_i^2/3$ and $\tau(i)\mathrm{d}\gamma < 0$, then

$$\mathrm{d}\tau(i) = G\mathrm{d}\gamma,\ \mathrm{d}\gamma^P(i) = 0, \tag{13}$$

and in the opposite case

$$\mathrm{d}\tau(i) = \frac{Gh\mathrm{d}\gamma}{\sqrt{6}G + h},\ \mathrm{d}\gamma^P(i) = \frac{\sqrt{6}G\mathrm{d}\gamma}{\sqrt{6}G + h}. \tag{14}$$

In Fig. 4, the dotted line represents the strain–stress curve calculated from Eqs. (13) and (14) for active loading, when $h = 345$ MPa. This value of h was optimal to obtain the above-mentioned small linear hardening observed on the test curve.

Figures 5 and 6 show the diagrams calculated for the case of reversed stress cycles of two amplitudes. After the hysteresis loop was practically stabilized on the first amplitude 112 MPa, the amplitude of cycling stress was increased to 120 (Fig. 5) or 123 MPa (Fig. 6). Then, cyclic hardening restarted. Figure 7 shows the strain–stress diagram for initial reversed stress cycles of the amplitude 120 MPa. According to these diagrams, the hysteresis loops are symmetrical with respect to zero strain if not all of the elements have plastic strains, otherwise the hysteresis loop would not be symmetrical to zero strain. For example, the whole hysteresis loop would then be located in the region of positive strains (Fig. 7). It should be noted that it is not possible to describe this nonsymmetry by adding supplementary elements with higher initial yield stresses to the C–B model.

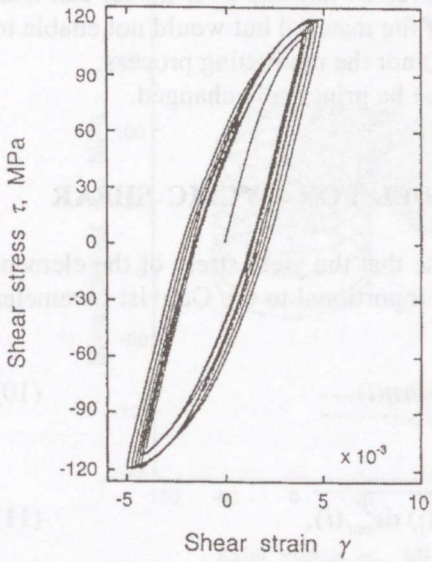

Fig. 5. Strain–stress diagram of reversed cycles of stress for two amplitudes: 112 and 120 MPa.

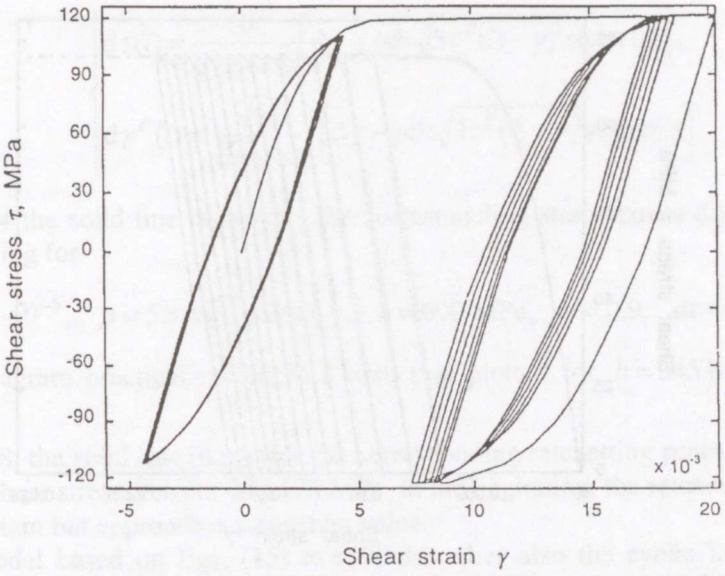

Fig. 6. Strain–stress diagram of reversed cycles of stress for two amplitudes, 112 and 123 MPa.

Such kind of nonsymmetry is a well-known property of many materials, proving that the described improvement of the model was necessary.

In Fig. 8, a strain–stress diagram is depicted for stress cycling from 0 to 120 MPa. It can be seen that in spite of the twenty applied cycles, no ratchetting takes place (dotted curve) and a steady state is reached at once.

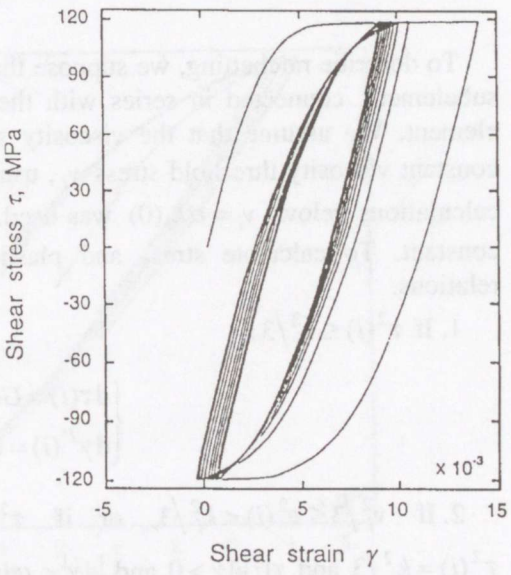

Fig. 7. Strain–stress diagram of reversed cycles of stress for amplitude 120 MPa.

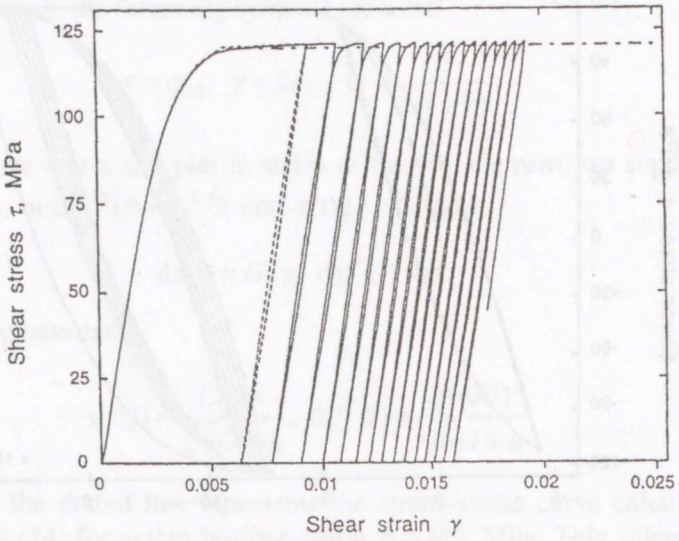

Fig. 8. Ratchetting for stress pulsation from 0 to 120 MPa: – · – C–B model, – – – model with isotropic hardening ($h = 345$ MPa), —— model with isotropic hardening ($h = 690$ MPa) and viscosity.

To describe ratchetting, we suppose that each element consists of a viscosity subelement, connected in series with the elastic and slip subelements of this element. We assume that the viscosity subelement of the ith element has a constant viscosity threshold stress v_i, usually different for each element. In the calculations below, $v_i = \alpha k_i(0)$ was used. Here α is assumed to be a material constant. To calculate stress and plastic strain, we propose the following relations.

1. If $\tau^2(i) \le v_i^2/3$:

$$\begin{cases} \mathrm{d}\tau(i) = G\mathrm{d}\gamma, \\ \mathrm{d}\gamma^P(i) = 0. \end{cases} \tag{15}$$

2. If $v_i^2/3 \le \tau^2(i) < k_i^2/3$, or if $\tau^2(i) = k_i^2/3$ and $\tau(i)\mathrm{d}\gamma < 0$, or if $\tau^2(i) = k_i^2/3$ and $\tau(i)\mathrm{d}\gamma > 0$ and $|\mathrm{d}\gamma| < \mu \mathrm{d}t\sqrt{3\tau^2(i) - v_i^2}$:

$$\begin{cases} \mathrm{d}\tau(i) = G\left[\mathrm{d}\gamma - \mu \mathrm{d}t\sqrt{3\tau^2(i) - v_i^2}\,\mathrm{sign}\,\tau(i)\right], \\ \mathrm{d}\gamma^p(i) = 0. \end{cases} \tag{16}$$

3. If $\tau^2(i) = k_i^2/3$ and $\tau(i)\mathrm{d}\gamma > 0$ and $|\mathrm{d}\gamma| > \mu \mathrm{d}t\sqrt{3\tau^2(i) - v_i^2}$:

$$\begin{cases} \mathrm{d}\tau(i) = \dfrac{Gh}{\sqrt{6}G + h}\left[\mathrm{d}\gamma - \mu \mathrm{d}t\sqrt{3\tau^2(i) - \nu_i^2}\,\mathrm{sign}\,\tau(i)\right], \\ \mathrm{d}\gamma^P(i) = \dfrac{\sqrt{6}G}{\sqrt{6}G + h}\left[\mathrm{d}\gamma - \mu \mathrm{d}t\sqrt{3\tau^2(i) - \nu_i^2}\,\mathrm{sign}\,\tau(i)\right]. \end{cases} \tag{17}$$

In Fig. 4 the solid line represents the corresponding strain–stress diagram in active loading for

$$|\mathrm{d}\gamma| = 2 \cdot 10^{-5}, \quad \mu = 5.8 \cdot 10^{-7}\ 1/\mathrm{MPa\,s}, \quad h = 690\ \mathrm{MPa}, \quad \alpha = 0.9, \quad \mathrm{d}t = 0.1\ \mathrm{s}.$$

This diagram practically coincides with that plotted for $h = 345$ MPa and $\mu = 0$.

In Fig. 8, the solid line illustrates the corresponding ratchetting process in the cycles of shear stress τ from 0 to 120 MPa. In the beginning, the ratchetting rate is not constant but approaches a constant value.

The model based on Eqs. (15) to (17) describes also the cyclic hardening process, as shown in Figs. 9 and 10. Again, the stabilized hysteresis loops are symmetrical with respect to zero strain if not all elements have plastic strains, and are nonsymmetrical in the opposite case.

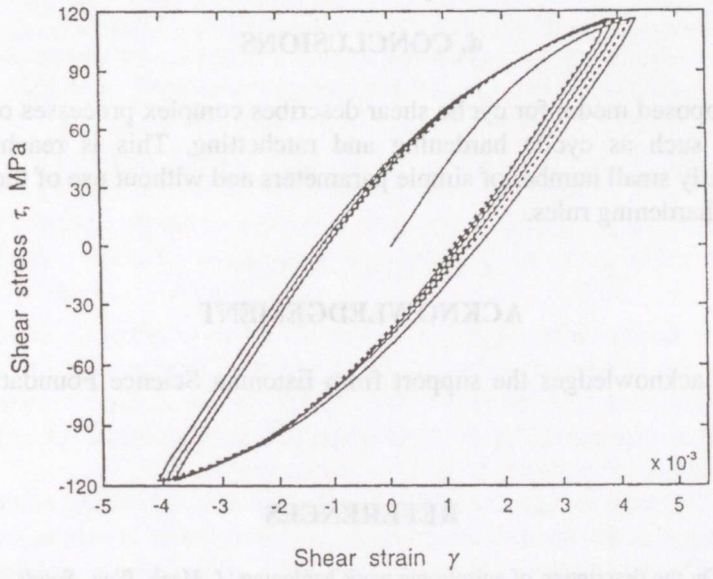

Fig. 9. Strain–stress diagrams of reversed cycles of stress for amplitude 114 MPa: – – – model with isotropic hardening (h = 345 MPa), —— model with isotropic hardening (h = 690 MPa) and viscosity.

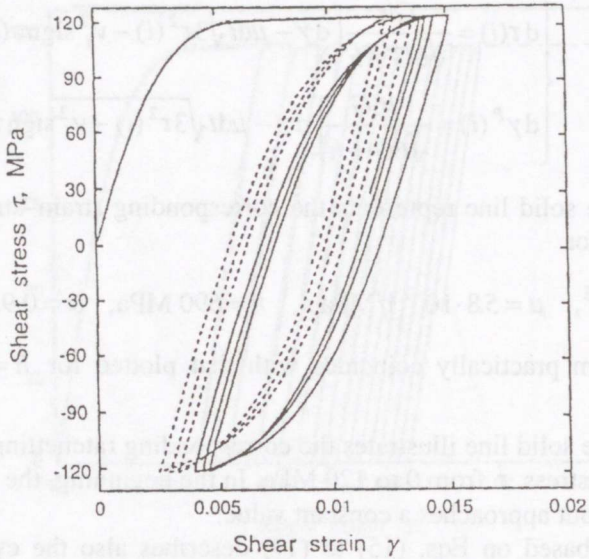

Fig. 10. Strain–stress diagrams of reversed cycles of stress for amplitude 122 MPa: – – – model with isotropic hardening (h = 345 MPa), —— model with isotropic hardening (h = 690 MPa) and viscosity.

4. CONCLUSIONS

The proposed model for cyclic shear describes complex processes of material behaviour such as cyclic hardening and ratchetting. This is reached by an exceptionally small number of simple parameters and without use of the complex kinematic hardening rules.

ACKNOWLEDGEMENT

Author acknowledges the support from Estonian Science Foundation, grant No. 1894.

REFERENCES

1. Mroz, Z. On the description of anisotropic work hardening. *J. Mech. Phys. Solids*, 1967, **15**, 3, 163–175.
2. Chiang, D. Y. and Beck, J. L. A new class of DEM for cyclic plasticity–I. Theory and application. *Int. J. Solids Struct.*, 1994, **31**, 4, 469–484.
3. Jiang, Y. and Sehitoglu, H. Modeling of cyclic ratchetting plasticity. *J. Appl. Mech.*, 1996, **63**, 3, 720–733.

TSÜKLILISE NIHKE MUDEL PLASTSUSTEOORIAS

Kalju KENK

Et kirjeldada tsüklilist nihet plastsusteoorias, on töös [2] esitatud mudelit (mudeli iga element loetakse selle elemendi pingeruumis ideaalselt plastseks) täiendatud järgmiselt: 1) mudeli element loetakse selle elemendi enda pingeruumis lineaarselt isotroopselt kalestuvaks sõltuvalt deformeerimise teepikkusest elemendi deformatsiooni ruumis ja 2) mudeli igasse elementi lisatakse viskoosne allelement, milles deformatsioonid arenevad ainult juhul, kui elemendi nihkepingete intensiivsus on suurem viskoossuslävest (viimane on üldjuhul igal elemendil erinev) ja elemendi viskoosse deformatsiooni kiirus postuleeritakse võrdeliseks ruutjuurega elemendi nihkepingete intensiivsuse ja viskoossusläve ruutude vahest. Need täiendused võimaldavad saadud mudeli abil kirjeldada ka materjalide tsüklilist kalestumist ja ühesuunalise plastse deformatsiooni kogunemist pulseerival koormamisel.